Soft Matter

RSC Publishing

PAPER

View Article Online
View Journal

Purified oleosins at air–water interfaces

Cite this: DOI: 10.1039/c2sm27118d

Constantinos V. Nikiforidis,*[ab] Christos Ampatzidis,[c] Sofia Lalou,[b] Elke Scholten,[a] Thodoris D. Karapantsios[c] and Vassilios Kiosseoglou[b]

Oleosins are low molecular mass proteins that are distinguished from other proteins for their extended central hydrophobic domain which covers almost half of its entity. For this work, they were extracted from isolated maize germ oil bodies. The purification steps included washing with diethylether and a chloroform–methanol–water mixture. Their amphipathic terminal domains positioned at the organelle surface, where they strongly interact with the surface polar phospholipids, made the application of a third washing step with acetone essential. Although oleosins are well known for their insolubility in water, we were able to prepare aqueous buffer solutions of 0.008 wt% at pH 8.0. The interfacial behaviour of oleosins was studied, in order to predict their ability to stabilize foams. Even at low concentrations they were capable of decreasing the interfacial tension of air–water interfaces to values similar to those obtained from milk protein or egg yolk apolipoproteins adsorption. Pendant drop profile analysis showed that the dilatational elastic modulus was frequency-dependent, but at the same time the elastic to viscous modulus ratio was frequency-independent and below 0.1. The results indicate that oleosins might have a high potential as foam stabilizers, a fast developing and challenging field.

Received 13th September 2012
Accepted 15th November 2012

DOI: 10.1039/c2sm27118d

www.rsc.org/softmatter

Introduction

Plant seeds subjected to desiccation store lipids, mainly triglycerides, in the form of distinct intracellular organelles called oil bodies[1] that serve as an energy storage place to support periods of active metabolism such as seedling growth during germination. One common feature of all oil bodies, irrespective of their origin, is the presence of a mixed phospholipid–protein membrane at their surface, responsible for maintaining oil body integrity.

Their mean diameter is between 0.1 and 3.0 μm and their size is probably affected by environmental factors and nutritional status.[2] Electron microscopy analysis suggests that the organelles consist of a central core of triglycerides surrounded by a single layer of phospholipids having the hydrophobic domain directed towards the oil body core and the hydrophilic head group exposed to the cytosol.[3] Depending on the plant origin, the phospholipid content may range between approximately 0.6 and 2%. In maize germ oil bodies the phospholipid content is about 0.9%.[4] The protein concentration of an oil body also differs between different sources and has been found to be in between 0.6 and 4.0%,[5] with oleosin, a unique protein, being the most abundant.

Oleosins are hydrophobic proteins with a molecular mass of about 15 to 26 kDa,[6] which completely cover the surface of the subcellular oil bodies, together with some minor proteins, called caleosins and steroleosins.[3,7–10] The ratio between the amount of oil and oleosin determines the size and sometimes the shape of the oil bodies. This can be best observed in maize germ, where due to the high oleosin-to-oil ratio the organelles are very small and irregularly shaped.[6] Oleosins adopt a unique conformation at the oil body surface, creating a membrane in which a large hydrophobic domain is flanked by hydrophilic domains facing the cytosol.[11] The hydrophobic domain is unique in the size of its uninterrupted hydrophobicity (72 residues) and is predicted to reside completely within the phospholipid layer and the oil triacylglycerols.

The hydrophobic domain was originally predicted to be an antiparallel strand with a turn mediated by the central "proline knot" motif.[2] However, recent studies on oleosins in the native oil body environment by Fourier transform infrared spectroscopy have indicated a predominance of an α-helical structure.[12] The hydrophobic domain is flanked by variable lengths and sequence N-terminal (N) and C-terminal (C) domains possess a significant amphipathic structure, which is expected to facilitate association with phospholipid surfaces.[13] Caleosins and steroleosins are larger in size, with a similar but smaller hydrophobic sequence and a less conserved proline knot sequence.

Oleosins, which up to now have found a number of biotechnological applications,[14,15] are predicted to behave in a

[a]Physics and Physical Chemistry of Foods, Wageningen University, P.O. Box 8129, 6700EV Wageningen, The Netherlands. E-mail: costas.nikiforidis@wur.nl; Fax: +31 317 483669; Tel: +31 317 483992

[b]Laboratory of Food Chemistry and Technology, School of Chemistry, Aristotle University, Thessaloniki, GR-54124, Greece

[c]Division of Chemical Technology, School of Chemistry, Aristotle University, Thessaloniki, GR-54124, Greece

similar manner to animal serum apolipoproteins[16] and can irreversible bind to the lipid–water interface.[17] Due to their well-known emulsification properties and the fact that they are natural products, their use could be of great interest to the food, cosmetic and pharmaceutical industry. Therefore, there are already some interesting studies about the interfacial properties of oleosin from rapeseed[18] or caleosin from *Arabidopsis thaliana*[19] combined with phospholipids.

Proteins play a very important role in emulsion stabilization, and recently, protein-stabilized foams have attracted considerable research interest due to their unique properties and potential technological applications.[20–23] To define whether a protein has a potential to act as a stabilizer for foams and emulsions, the adsorption dynamics and dilatational rheology of the formed interfacial layers are important. There are three major destabilizing mechanisms in foams: *drainage* of liquid from Plateau borders and nods between bubbles, bubbles *coalescence* and bubbles *disproportionation* (also known as *coarsening*). For food foams where the liquid volume fraction is relatively high (~above 0.1), in order to yield taste and texture in the mouth, drainage is usually the dominant destabilization mechanism right after the production of foams. Initial liquid drainage in wet foams has small relevance with the bubble size distribution in the foam.[24,25] However, the long lasting performance of such wet foams is also dictated by coalescence and disproportionation since the latter affects the bubble size distribution and, therefore, the number and size of Plateau borders and nods in the foam.

Dynamic surface tension measurements illustrate the adsorption kinetics of molecules to interfaces under strain, *e.g.* value of diffusion coefficients, existence of steric or electrostatic barriers, *etc.* Yet, dynamic surface tension cannot provide information on the relaxation processes occurring within the adsorpted layer. This can be done by measurements of interfacial viscoelasticity. Interfacial dilatational and shear viscoelasticity, or quite often the surface dilatational modulus, are found to be associated with the macroscopic dynamics of multiphase systems.[26] During liquid drainage in foams, bubble interfaces are primarily sheared whereas during bubble coalescence and disproportionation interfaces are primarily dilated.

In the most general case, any disturbance of an interface initiates both elastic and viscous effects that can be described by an interfacial dilatational modulus. In compression/expansion of an interface the interfacial dilatational modulus E_d is defined as the change in surface tension γ for a small relative change in surface area A.[27,28] In a system of two equally sized bubbles of which one will grow and the other will dissolve due to a Laplace pressure difference, when a bubble decreases in size, the surface tension, γ, decreases as a result of an increase in surface load. Similarly, the bubble pressure, P, increases when the size decreases.

$$E_d = -\frac{dP}{d\ln A} = \frac{d\gamma}{d\ln A} \quad (1)$$

Stabilization occurs if the change in bubble pressure due to a change in radius, $d\Delta P/dR$, is larger than 0. The combination with the definition for the Gibbs elastic dilatational modulus, E_d, leads to the conclusion that for a completely elastic interface, the driving force for bubble stability is maintained when the elastic dilatational modulus is larger than half the surface tension.

$$\frac{d\Delta\Pi}{dR} = \frac{d\left(\frac{2\gamma(R)}{R}\right)}{dR} = -\frac{2\gamma}{R^2} + \frac{4E_d}{R^2} > 0; \quad E_d > \frac{\gamma}{2}, \quad \frac{2E_d}{\gamma} > 1 \quad (2)$$

From a practical point of view it is a challenging task to find surface active materials which rapidly adsorb to an interface, providing good foamability and stability against early stage bubble coalescence and disproportionation. This interest has led to studies on the behaviour of novel natural emulsifiers, like hydrophobins,[29] saponins[30] and particles.[31,32]

A well-known protein that has been extensively studied both as an emulsifier and as a foaming agent is β-casein.[33] Its high surface activity is ascribed to its small size (24 kDa), hydrophobicity and high flexibility. Oleosin molecules originating from maize germ are also very hydrophobic[34] while their size is even smaller than caseins. Considering the protein structure, it could be more flexible than that of casein. Therefore, it may be useful as an emulsifier or foaming agent. In the present work, we apply equilibrium surface tensiometry and drop profile analysis to investigate the equilibrium and dynamic properties of oleosin at the air–water interface. In the experiments, proteins of highest purity were used, by optimizing the oleosin extraction from maize germ. The isolation of oleosins is based on a protocol of oil body extraction which we followed in a previous research study.[35]

Experimental section

Materials

A milling industry by-product, rich in maize germ, was used for the aqueous extraction of oil bodies. All other chemicals were obtained from Sigma-Aldrich Co., LLC.

Oil body extraction

The oil bodies were isolated using an aqueous extraction method (Fig. 1).[35] The intact germs were first collected by hand and then subjected to comminution, using a Brown mill fitted with knives, to pass through a 0.8 mm mesh sieve. The germ flour was initially soaked in deionised water (20% w/v) and the pH was adjusted and kept constant at 9.0, using a 0.1 M NaOH solution, while continuously agitating for 24 h with the use of a mechanical stirrer (Kika Labortechnik, Malaysia), at 1200 rpm. The mixture was then subjected to intensive agitation (speed set at position 2) for 40 s, by employing a Braun Blender (Type: 4249, Germany), and the resulting dispersion was filtered through a filter made up of three layers of cheesecloth. The germ residue was then again extracted with deionised water at pH 9, the two oil body dispersions containing both oil bodies and debris were combined into one and the pooled dispersion was subjected to centrifugation (Firlabo SV11, France) at 3800*g* for 20 min to remove insoluble solids. The recovered oil body dispersion was then mixed with an equal volume of a sucrose

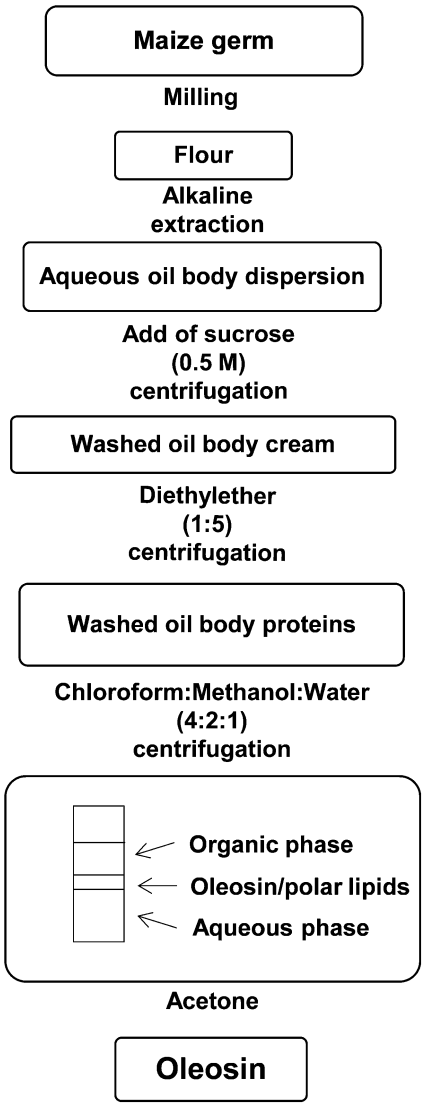

Fig. 1 Diagram of the extraction and purification steps of maize germ oleosins.

solution (pH 6.5) to obtain a final sucrose concentration of 0.5 M and the diluted dispersion was centrifuged at 3800*g*. The cream at the top was then recovered and washed once more with the sucrose solution. Moisture, fat and protein contents were determined according to the standard methods of AOAC.[36]

Oleosin extraction and purification

Oleosins were extracted from isolated oil bodies (Fig. 1). First, 5 volumes of diethylether were added to 1 volume of oil body cream, following centrifugation at 5000*g* for 15 min. The organic upper phase was discarded and the washing step was repeated another 4 times. Then, chloroform–methanol was added, in order to form a chloroform–methanol–water mixture with a 4 : 2 : 1 ratio. After centrifugation (5000*g*, 15 min), the intermediate layer of white material was collected and resuspended in chloroform–methanol–water (4 : 2 : 1) and centrifuged (5000*g*, 15 min). The intermediate white layer was collected and freeze-dried, after the evaporation of the remaining organic solvent under nitrogen and then analysed with SDS-PAGE. The same procedure was followed for the upper methanol–water and the lower chloroform layer.

The freeze-dried material was resuspended in acetone and after centrifugation (5000*g*, 15 min), the precipitate was collected using small amounts of water. The last step was repeated twice and, finally, the aqueous protein suspension was freeze-dried and the remaining powder was analysed using SDS-PAGE.

Protein analysis

The extracted and purified material was analysed by SDS-PAGE[37] using 4.5 and 12.0% v/w acrylamide solutions for the stacking and separating gels, respectively. The oil body samples were treated with a 0.0625 M Tris buffer containing 2% w/v SDS, 10% w/v glycerol, 0.1% w/v bromophenol blue and 5% β-mercaptoethanol. After boiling for 2 min and the application of two freeze–thaw cycles, the subnatant containing the protein was recovered by centrifugation and applied onto the electrophoresis gel. Protein fractions were fixated by immersing into a 12.5% w/v trichloroacetic acid solution. The gels were stained with Coomassie brilliant blue G-250 and photographed with the aid of a digital camera (Kodak DC3400). Determination of the protein molar mass was performed with the aid of the Electrophoresis Programme Gel Pro.

The amount of non-aggregated protein material that was still solubilized in the aqueous buffer solution after centrifugation at 16 000*g* (4 °C, 30 min) was determined colorimetrically using the Modified Lowry protein assay.[38]

Zeta potential measurements

The zeta potential was measured by a dynamic light scattering apparatus (DLS Zetasizer NanoZS, Malvern Instruments Ltd, Worcestershire, United Kingdom) which was equipped with an autotitrator (MPT-2 Autotitrator, Malvern Instruments Ltd, Worcestershire, United Kingdom) in order to measure zeta potential as a function of pH. The protein samples were dissolved in a 20 mM Tris buffer with a pH of 8.0. Milli-Q water was used to prepare the buffer.

Equilibrium surface tension measurements

Equilibrium surface tension values were determined by a LAUDA TE2 tensiometer furnished with a Wilhelmy plate made of Pt/Ir (90/10). The instrument was calibrated against standard pure liquids and Millipore water. Agreement with literature values was typically within ±0.1 mN m^{-1}. Specific cleaning procedures were performed for the plate and the experimental vessel. Measurements were taken at approximately 4 h after the plate was immersed in the solution, which was a time interval always adequate to reach a final steady value (±0.5 mN m^{-1}) at $T = 25 \pm 0.1$ °C. Three records are acquired at all experimental conditions and standard deviations are less than 0.3 mN m^{-1}.

Dynamic surface tension measurements

Dynamic surface tension measurements were performed with a drop profile analysis tensiometer (PAT-1S, SINTERFACE). The

principle of this method is to determine the instantaneous surface tension of the studied solution from the shape of a pendant drop. Due to the active control loop, the instrument allows long-time experiments keeping the volume of the measuring drop constant. In this study we used a pendant drop ($V = 12$ mm^3) formed at the tip of a stainless capillary with a diameter of 3 mm. The temperature of the measuring glass cell was kept constant at $T = 25 \pm 0.1$ °C. Three repeatability checks are made for each set of conditions. Pearson correlation coefficients among sampled curves are always above 0.93 whereas standard deviations at equal adsorption times are less than 0.3 mN m^{-1}.

The experimental data of time-dependent interfacial tension were analysed by fitting the data to the following equation:

$$\gamma(t) = \gamma_\infty + \gamma_1 e^{-t/t_1} + \gamma_2 e^{-t/t_2} \quad (3)$$

On the right hand side of the equation, γ_∞ represents the surface tension at an equilibrium state whereas the two exponential terms correspond to the two distinct relaxation processes. For proteins and other macromolecules it is customary assumed that the first exponential decay of surface tension describes the relatively fast stage of molecules adsorption to the gas–liquid interface while the second exponential decay describes the slower stage of molecules rearrangement at the interface. Non-linear numerical fitting of eqn (3) to experimental data was achieved by the Levenberg–Marquardt method[39,40] using MATLAB software (MathWorks).

Dilatational viscoelasticity

Dilatational surface rheology measurements provide information on the dynamic activity of the adsorbed surface layer and are especially sensitive to conformational transitions in adsorption layers. For surface area variations at moderate rates of deformation, the ability of a surfactant to relieve stress is limited by adsorption or desorption from or to the bulk solution, and as a result, relaxation processes come into play, leading to gradual re-equilibration of the system.

The surface dilatational modulus E_d depends on the frequency of surface deformation and can be presented as a complex number:

$$E(\omega) = E_r(\omega) + iE_i(\omega) \quad (4)$$

The real part $E_r(\omega)$ is the storage modulus representing the recoverable elastic energy stored in the surface (dilatational elasticity) whereas the imaginary part $E_i(\omega)$ is the loss modulus reflecting the viscous dissipation of energy through any relaxation (time-dependent) processes at or near the surface (dilatational viscosity). Although such measurements can, in principle, be performed to characterize the instantaneous adsorbed surface layer even at times prior to equilibration, surface rheology properties at equilibrium are of primary concern.

The complex surface dilatational modulus is measured by an oscillating drop profile analysis (ODPA) technique using a dedicated mode of the drop profile tensiometer (PAT-1S Sinterface). Analysis of data is carried out on the basis of a simple rheological model (Maxwell) using just one relaxation frequency. This approach assumes that the relaxation frequency and the intrinsic elastic modulus of the adsorption layers are independent of the applied oscillation frequency. The apparatus and operational procedures are described in detail elsewhere.[41] As described in Section 2.7, a pendant drop is created at the tip of a capillary by a computer driven dosing system in a sealed glass cuvette. The software allows controlling the surface volume of the drop as a function of time and thus imposing harmonic oscillations of the drop volume. The employed volume oscillation amplitude is 5% of the initial drop volume. The employed oscillation frequencies are 0.001, 0.005, 0.01, 0.02, 0.05, 0.1 and 0.2 Hz. Measurements are taken after at least 20 000 s of adsorption (end of dynamic surface tension measurements) where the adsorption layer is under quasi-equilibrium conditions. Three repeatability checks are made for each set of conditions. Standard deviations in the storage modulus and loss modulus are less than 0.3 mN m^{-1}.

Results and discussion

Extraction of maize germ oil bodies

To remove the co-extracted, non-interfacial proteins from the maize germ oil body aqueous dispersion,[42] a sucrose solution was added, followed by a centrifugation step.[35] According to the literature, treatment with urea was necessary to remove the extraneous proteins from sunflower oil bodies,[43] but trials with maize germ oil bodies did not have the expected results. In fact, extensive treatment with 9.0 M urea resulted in the partial removal of the non-interfacial proteins (data not shown). The ratio between oil and proteins in the pure oil bodies was around 30 : 1. The interfacial protein fraction consisted mainly of oleosin, but small amounts of caleosin and steroleosin were present as well.[35] Therefore, in order to determine the interfacial behaviour of oleosin molecules these proteins had to be separated from the other interfacial protein fractions.

Purification and characterization of oleosins

The cream of washed oil bodies (moisture: 46.7%; crude fat: 44.9%; total protein: 1.6%, $N\% \times 5.7$) was extracted with diethylether (1 : 5) to remove the neutral lipids. After each centrifugation step, the protein material formed a whitish interfacial layer between the water and the organic solvent. This layer probably consisted of interfacial oil body proteins, mainly oleosins, but also others were present. The extraction and purification of oleosins from this mixture were based on a modification of a protocol, which was first applied by Ferro *et al.*[44] According to these researchers, the hydrophobicity of proteins determines their solubility in chloroform–methanol mixtures. Caleosins and steroleosins are less hydrophobic than oleosins,[8,45] so mixing of the organic solvents with deionised water at different ratios could lead to their fractionation. The effective separating ratio between the solvents (chloroform–methanol–water) was found to be 4 : 2 : 1. By using this extraction ratio, caleosins and steroleosins ended up in the

lower organic solvent (as analysed with SDS-PAGE) and at the interface a powder was found with a very low affinity for both organic and aqueous solvents. This was expected to be the fraction consisted of oleosins, since these proteins did not appear in the SDS-PAGE electropherograms of the organic and aqueous solvents. Electrophoretic analysis of the material at the interface with SDS-PAGE showed that besides the expected oleosins a protein with a molecular mass below 10 kDa was also at the interface. This fraction was of a molecular mass much lower than that of maize germ oleosins which has been found to be around 15–17 kDa.[35,46] It is well known that when oleosins are at the oil body interface they strongly interact with the interfacial polar phospholipids.[47] In case they were not successfully washed during the application of the purification steps, they might have an influence on the protein molecular mass of the SDS-PAGE electropherogram.[48] To investigate whether phospholipids were still attached to oleosins, a third washing step was necessary. The freeze dried intermediate material was washed two times with small volumes of acetone, which can solubilize polar lipids. After evaporating the organic solvent under N_2, distilled water was used to recover the remaining solid material from the vessel, which was removed in the next step using a freeze dryer. SDS-PAGE analysis showed a single band around 16 kDa (Fig. 2), which could be attributed to the oleosin fraction. These results indicate that at the oil body interface, proteins are embedded in a layer with phospholipids, where strong electrostatic interactions between the proteins and the polar lipids take place. In order to purify oleosins the washing step with acetone appears to be essential.

ζ-Potential measurements

According to previous studies,[35] the washed extraneous protein oil bodies have an isoelectric point between 4.5 and 5.0. It would be interesting to investigate whether this charge is only due to the protein fractions or to the combination of the charged phospholipids with the proteins. The influence of the changes in the environmental pH on the protein charge of the oleosin fraction is shown in Fig. 3. In the absence of phospholipids and the other interfacial protein fractions (caleosins and steroleosins), oleosins seem to have a slightly higher positive charge, with a p*I* value slightly higher than 5. This difference in the ζ-potential can be attributed to the interactions between the phospholipids and oleosins, which may be attributed to the charge and polarity distribution within the molecules. An oleosin molecule carries a total of about 5 positive charges. The orientation of the oleosin molecules on the oil body interface is such that the negative charges are exposed to the cytosolic side of the oil body and the positive charges face the interior.[2] These positive charges interact at the surface with negatively charged phospholipids. The negatively charged phospholipids, representing around 0.3% of the total mass, partition themselves at the oil body interface.

For the purified oleosins, the absence of polar lipids might have an important influence on the intermolecular interactions and the tertiary structure of the protein molecule. Thus, oleosin is expected to have a different structure in an aqueous solution and different arrangement in an air–water interface. Their structure is expected to be different from the model that was first suggested by Qu and Huang[49] with regard to the arrangement of maize germ oleosin molecules at the oil body surface.

Oleosin solubility in aqueous environment

Oleosin molecules have a very extensive central hydrophobic domain with 72 residues,[2] thus when they are found in a "non-friendly" aqueous environment they probably tend to form aggregates. According to Roux *et al.*[50] it was not possible to solubilize oleosins from *Arabidopsis thaliana* in an aqueous solution, therefore they solubilized the protein in 8.0 M urea and suspended the solution in sunflower oil. Another research group[18] dispersed the protein molecules in the oil phase, which, in this case, was triolein, in order to measure the interfacial behaviour of rapeseed oleosins. The only time that a dispersion of oleosins in an aqueous environment was reported was in combination with anionic detergents or amphipols.[51]

According to the literature[52] the formation of protein aggregates has a big influence on the foaming activity, so the aim of this research was to measure the air–water interfacial behaviour

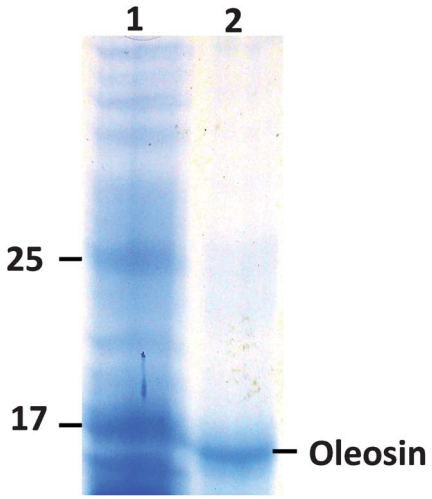

Fig. 2 SDS-PAGE profiles of purified oleosin (lane 2) and molecular mass markers (lane 1).

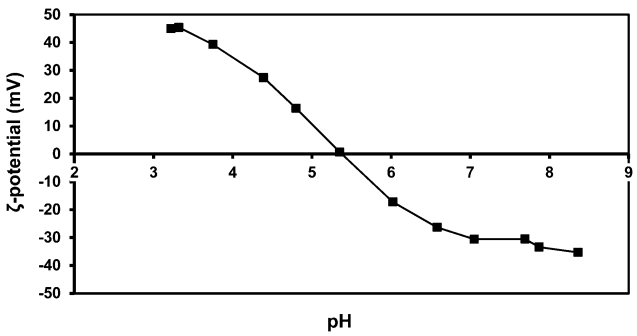

Fig. 3 Dependence upon pH of the ζ-potential of oleosin molecules originating from maize germ.

of the individual purified protein molecules. Hence, an aqueous buffer solution at pH 8.0 was used as a dispersant. At this pH the ζ-potential was larger than −30 mV (Fig. 2) and the molecules were expected to repel each other. However, in spite of the increased charge of the molecules, the appearance of hydrophobic interactions could again lead to protein aggregation. In order to avoid the presence of flocs, which could influence the interfacial behaviour measurements, the oleosin solution was centrifuged at high speed to separate the aggregates and the precipitate was discarded. The concentration of the protein molecules remaining in the aqueous buffer and presumably not aggregated was determined using a photometric technique. Following this procedure the concentration of the individual protein molecules was found to be 0.008 wt%, and therefore the measurements of the interfacial behaviour of oleosins were possible only at low concentrations.

Equilibrium and dynamic surface tension

The interfacial activity of oleosins at air–water interfaces after equilibration for 4 hours was first measured using a tensiometer furnished with a Wilhelmy plate. Roux *et al.*[50] suggested that oleosins in the absence of phospholipids are not capable of inserting themselves at air–water interfaces but Fig. 4 demonstrates that purified maize germ oleosins were surface active shifting surface tension to lower values. Those researchers could have these negative results due to the method they applied for purifying the proteins which might have led to changes in their structure that in turn influenced their functionality. According to the present results, oleosins are surface active even at very low concentrations (0.002 wt%) and surface tension decreases further when the protein concentration of the aqueous solution is increased. The lowest values of surface tension were observed at a protein concentration of 0.008 wt%, but a plateau was not yet reached, which indicates that at this concentration there were not enough molecules to cover the surface completely. A similar decrease in surface tension values, measured with a DuNouy platinum ring, was also observed with calcium and sodium caseinates. As mentioned in the Introduction, oleosins are predicted to behave similarly to animal apolipoproteins. This similarity can also be observed when comparing the surface activity of oleosins with egg yolk.[53] The presence of liquid yolk yields a decrease of surface tension (or an increase of surface pressure), which is equal to those found for the oleosin solution.

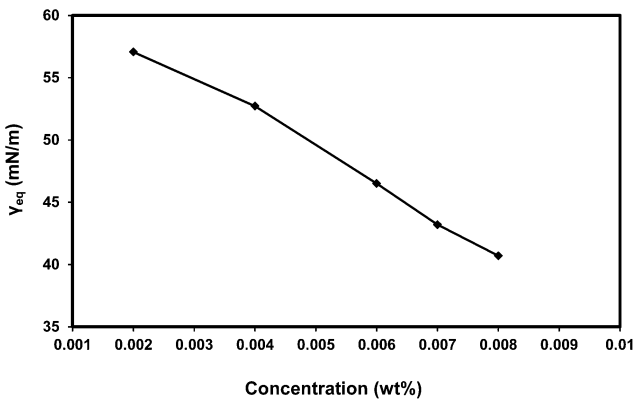

Fig. 4 Equilibrium surface tension ($\gamma_{eq.}$) *versus* oleosin concentration ($T = 25\ ^{\circ}C$).

Pendant drops of protein aqueous solutions were formed in order to investigate the influence of the protein bulk concentration on the dynamic surface tension at air–water interfaces (Fig. 5). As it can be observed, the dynamic surface tension measurements illustrate the adsorption kinetics of molecules to interfaces, *e.g.* diffusion to sublayer, existence of steric or electrostatic barriers, limiting values for short and long adsorption times, *etc.* In the examined surface age range, surface tension decreases and gradually levels-off at final values that vary with bulk concentration. Levelling-off occurs faster and the final values are lower as protein concentration increases. However, these final values are higher than the equilibrium values measured with the Wilhelmy technique at the same bulk concentrations. Thus, equilibrium is not reached with pendant drops even at long times. The discrepancy between the two techniques is not uncommon and is a result of the higher ratio of surface area-to-bulk volume for a drop geometry compared with the same ratio for the flat geometry of the Wilhelmy technique.

Experimental data in Fig. 5a were fitted fairly well by eqn (3), as is shown in Fig. 5b, which displays an example of the best-fitted theoretical curve derived from eqn (3) and the experimental data points for a protein concentration of 0.002 wt%. Table 1 shows the results of the best fit of eqn (3) through the experimental data points of all concentrations used. The table gives the characteristic relaxation times t_1 and t_2, and the residual standard error. It can be seen that both relaxation times t_1 and t_2 are sufficient in describing surface tension decay with time and are of the same order of magnitude. This implies that both molecule adsorption and rearrangement at the interface have appreciable contributions to the dynamic surface tension. The data show that, in general, both relaxation times (adsorption and rearrangement) decrease when the protein content increases.

The non-monophasic process can be clearly observed by plotting the graph with time at a logarithmic scale (Fig. 5c). According to this graph, there exist a first idle phase of molecules diffusion (I), (surface tension is essentially constant at the solvent value as protein molecules have not yet reached the interface) with a duration depending on the protein concentration, a second phase of adsorption (II) and a third phase of rearrangement and equilibrium (III). The intermittent lines in the figure divide the three phases when the protein bulk concentration is 0.004 wt%. Fig. 5a and b show that the three phases have different durations between different concentrations. Phase III is longer, when the protein concentration is higher, a fact which maybe indicates that the molecules at the interface are close enough and show significant interactions during rearrangement, increasing with concentration.

Similar adsorption kinetics were also reported for sodium caseinates adsorption at air–water interfaces[33] and for caleosins and oleosins from *Arabidopsis thaliana* at air–water and oil–water interfaces.[19,50] Deleu and co-workers measured the adsorption kinetics of oleosins from rapeseeds at triolein–aqueous

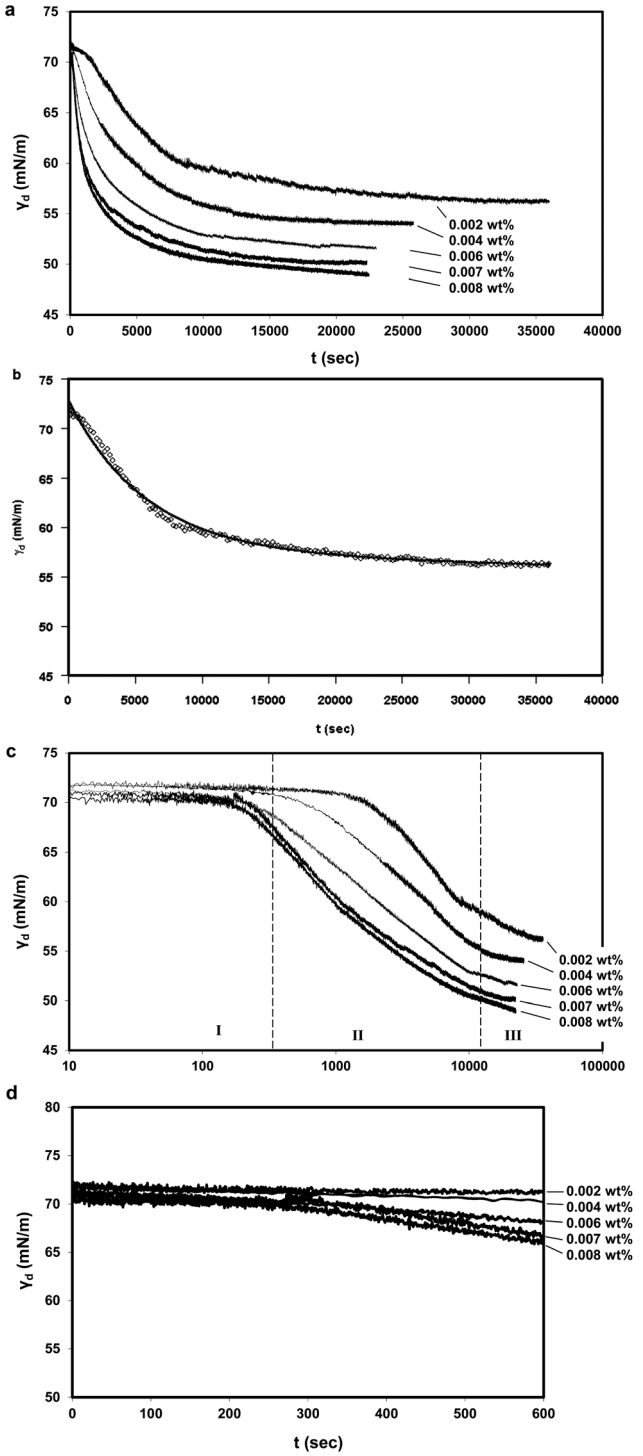

Fig. 5 Dynamic surface tension (γ_d) measurements (a and d) as a function of time (surface age) at various concentrations of oleosin, and (c) expressed using a time logarithmic scale. I, II and III indicate the three phases of diffusion, adsorption and finally rearrangement and equilibrium. (b) Comparison of the experimental data of the dynamic surface tension when the oleosin concentration is 0.002 wt% (◇) with the theoretical curve plotted using eqn (3) (—) ($T = 25$ °C).

interfaces[18] where according to the writers, in the absence of phospholipids, the adsorption kinetics of oleosins exhibit an almost linear behaviour. When oleosins were dispersed in triolein, the surface tension decreased instantaneously,

Table 1 Relaxation times and residual standard error at different oleosin concentrations

C (wt%)	t_1 (s)	t_2 (s)	Residual standard error (18 995 degrees of freedom)
0.002	5368	8331	0.301
0.004	3265	4812	0.163
0.006	4147	5908	0.519
0.007	2385	3385	0.234
0.008	885	3054	0.584

reaching equilibrium in about 50 s. This rapid adsorption was not observed for oil–water interfaces, where the interfacial tension decreased very fast during the first 100 s, but the equilibrium state was not reached before 3600 s.[50] These results are opposite to our findings, where more than 500 s are required to observe a marked change in the surface tension (Fig. 5d) and more than 10 000 s to approach the equilibrium state. The adsorption kinetics of our oleosin systems at air–water interfaces was similar to that of caleosins at the same interface[19] with the main difference being that oleosins exhibit a much higher surface activity, which is probably due to the higher hydrophobic character.

Surface elasticity and viscosity

Plots of the elastic modulus, E', and of the loss modulus, E''_d, *versus* angular frequency at different bulk oleosin concentrations are shown in Fig. 6a. Measurements were performed using a drop profile tensiometer. Depending on the protein concentration, the elastic modulus values ranged from 25 to 35 mN m^{-1} before oscillation started. These values were similar to those obtained for β-lactoglobulin and β-casein.[54] The corresponding loss modulus values, E''_d, of our systems were found to be very low, namely, below 5 mN m^{-1}. Both moduli showed high frequency dependence for all examined concentrations. Invoking a simple rheological model with one relaxation frequency, *e.g.*, the Maxwell model, the aforementioned frequency dependent behaviour is typical for a non-Newtonian viscoelastic interface. The peak value for the elastic moduli at ~0.03 s^{-1} indicates possible structural changes in the adsorption layer around this strain rate.[55] The monotonic decrease of the loss modulus values, E''_d, with oscillation frequency indicates a shear-thinning or pseudoplastic behaviour.

According to the literature,[56–58] an increase in the deformation rate of a drop interface has either no influence or may lead to an increase of E'_d for air–water surfaces stabilized with proteins. A decrease of the elastic moduli has only been reported when BSA was used to stabilize an oil–water interface, when the oil viscosity was very high.[59] This change of the interfacial dilatational elasticity could indicate that there are no extensive interactions present between the protein molecules at the surface and under oscillations the interfacial film collapses. This conclusion does not, however, correspond to the behaviour of the loss tangent (tan δ defined as E''_d/E'_d) (Fig. 6b) that shows values of almost always below 0.1 and exhibits a very low frequency dependence. The low E''_d/E'_d ratio indicates an almost

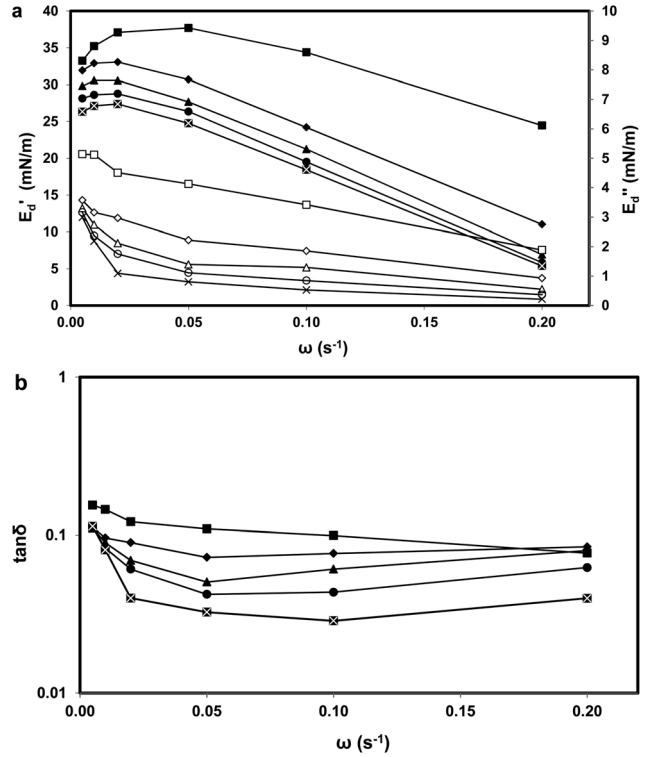

Fig. 6 (a) Interfacial dilatational elastic E_d' (black symbols) and viscous E_d'' (white symbols) moduli and (b) loss tangent as a function of oscillation frequency and oleosin concentration: (■ and □) 0.002 wt%; (◆ and ◇) 0.004 wt%; (▲ and Δ) 0.006 wt%; (● and ○) 0.007 wt%; (⊠ and ×) 0.008 wt% ($T = 25$ °C, amplitude: 5% of the initial drop volume).

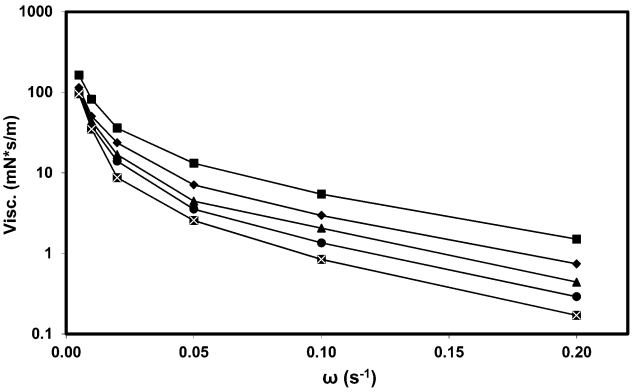

Fig. 7 Dilatational viscosity as a function of oscillation frequency and oleosin concentration: (■) 0.002 wt%; (◆) 0.004 wt%; (▲) 0.006 wt%; (●) 0.007 wt%; (⊠) 0.008 wt% ($T = 25$ °C, amplitude: 5% of the initial drop volume).

rubbery surface for which the surface elasticity provides a much greater contribution to the dilatational modulus than surface viscosity. This behaviour could be ascribed to oleosins elastic entanglement during compression and expansion of the interface where the kinetic energy is largely restored after each oscillation rather than dissipated by viscous molecular rearrangement. This behaviour could be attributed to the interactions between the protein molecules which are induced from the recurring expansion–compression steps. Oleosins have a large central hydrophobic domain, which comes into contact with a not so hydrophobic environment (air), and as a result the application of oscillations could lead to hydrophobic intermolecular interactions.

The interfacial dilatational viscosity *versus* oscillation frequency at different protein concentrations is shown in Fig. 7. As expected, the interfacial dilatational viscosity decreased with an increase in frequency. At very low frequencies the viscosity at all concentrations was almost the same, but an increase in the oscillation rate resulted in a higher decrease of viscosity at higher protein concentration. These results can again be explained by the hydrophobic interactions induced as a result of the application of oscillation. A higher protein concentration leads to more hydrophobic intermolecular interactions.

To exploit the surface rheological parameters in understanding the stabilization against disproportionation in foams, the factor, $2E_{max}/\gamma_{max}$, can be used, which, according to the Gibbs criterion, should be larger than 1.[27] It is worth mentioning that when making predictions towards bubble stabilization, it is assumed that deformation of the surface is purely elastic. However, all material deformation is a combination of elastic and viscous contributions. Computer simulations showed that in order to form stable bubbles against shrinkage, $2E_{max}/\gamma_{max}$ should be higher than 5 instead of the predicted theoretical value of 1.[60] For oleosins, the values of this ratio are between 1 and 2, which, according to the theoretical prediction, should be enough to stabilize the systems. These values are also found for β-lactoglobulin, which is a protein with a well-known ability to form stable foams.[61] According to the model of Kloek *et al.*[60] these values predict retardation of bubble shrinkage but no complete arrest. Finally, it must also be noted that according to this ratio β-casein should have no foamability, since according to Blijdenstein *et al.*,[56] $2E_{max}/\gamma_{max}$ is lower than 1, which is against the primary Gibbs criterion. However, foams with caseins have shown to be stable. Therefore, the practical implications of this theory should be taken with caution.

Conclusions

In this work we have studied the ability of oleosin, a protein with a small molecular mass and high hydrophobicity, to stabilize air–water interfaces. Oleosins are a unique group of proteins with an extensive central hydrophobic domain (72 residues). In nature they exist at the surface of oil bodies, embedded in a layer with phospholipids, structures which can be compared with milk fat droplets. Oil bodies and subsequently oleosins can be found in almost all seeds rich in oil. The stability of oil bodies is associated with the concentration of oleosins, therefore it is important to gain more knowledge about the mechanism of stabilization which could lead to future applications.

The surface properties of purified oleosins at an equilibrium state can be compared to the properties of milk proteins and egg yolk apolipoproteins. Higher oscillation frequency results in a decrease of the elastic dilatational modulus (E_d), but at the same time the loss tangent shows very low values (<0.1) and

remains almost constant, which probably indicates the formation of a strong elastic film at the surface, a fact that might make oleosins a good source for foaming agents.

The aim of this work was the understanding of the behaviour of purified individual oleosin molecules at air–water surfaces; therefore extensive washing steps were followed. It would be interesting to investigate the surface properties of oleosins before the last washing step with acetone. As mentioned before, oleosins are present at the surface of oil bodies, where they are embedded in a phospholipid layer and strong interactions between the protein molecules and the polar lipids occur, forming a complex. It might be possible that these complexes exhibit higher surface activity, but further research would be required.

References

1 G. Wanner, H. Formanek and R. R. Theimer, *Planta*, 1981, **151**, 109–123.
2 A. H. C. Huang, *Annu. Rev. Plant Physiol. Plant Mol. Biol.*, 1992, **43**, 177–200.
3 G. I. Frandsen, J. Mundy and J. T. C. Tzen, *Physiol. Plant.*, 2001, **112**, 301–307.
4 M. C. M. Chen, C. L. Chyan, T. T. T. Lee, S. H. Huang and J. T. C. Tzen, *J. Agric. Food Chem.*, 2004, **52**, 3982–3987.
5 J. T. C. Tzen and A. H. C. Huang, *J. Cell Biol.*, 1992, **117**, 327–335.
6 K. Hsieh and A. H. C. Huang, *Plant Physiol.*, 2004, **136**, 3427–3434.
7 L. J. Lin, S. S. K. Tai, C. C. Peng and J. T. C. Tzen, *Plant Physiol.*, 2002, **128**, 1200–1211.
8 L. J. Lin and J. T. C. Tzen, *Plant Physiol. Biochem.*, 2004, **42**, 601–608.
9 H. Tnani, I. Lopez, T. Jouenne and C. M. Vicient, *J. Plant Physiol.*, 2011, **168**, 510–513.
10 M. Vermachova, Z. Purkrtova, J. Santrucek, P. Jolivet, T. Chardot and M. Kodicek, *Proteomics*, 2011, **11**, 3430–3434.
11 B. M. Abell, L. A. Holbrook, M. Abenes, D. J. Murphy, M. J. Hills and M. M. Moloney, *Plant Cell*, 1997, **9**, 1481–1493.
12 D. J. Lacey, N. Wellner, F. Beaudoin, J. A. Napier and P. R. Shewry, *Biochem. J.*, 1998, **334**, 469–477.
13 M. Li, L. J. Smith, D. C. Clark, R. Wilson and D. J. Murphy, *J. Biol. Chem.*, 1992, **267**, 8245–8253.
14 S. C. Bhatla, V. Kaushik and M. K. Yadav, *Biotechnol. Adv.*, 2010, **28**, 293–300.
15 N. J. Roberts, R. W. Scott and J. T. C. Tzen, *Open Biotechnol. J.*, 2008, **2**, 13–21.
16 L. B. Wang, D. D. O. Martin, E. Genter, J. J. Wang, R. S. McLeod and D. M. Small, *J. Lipid Res.*, 2009, **50**, 1340–1352.
17 D. M. Small, L. B. Wang and M. A. Mitsche, *J. Lipid Res.*, 2009, **50**, S329–S334.
18 M. Deleu, G. Vaca-Medina, J. F. Fabre, J. Roiz, R. Valentin and Z. Mouloungui, *Colloids Surf., B*, 2010, **80**, 125–132.
19 Z. Purkrtova, C. Le Bon, B. Kralova, M. H. Ropers, M. Anton and T. Chardot, *J. Agric. Food Chem.*, 2008, **56**, 11217–11224.
20 A. Moro, G. D. Baez, P. A. Busti, G. A. Ballerini and N. J. Delorenzi, *Food Hydrocolloids*, 2011, **25**, 1009–1015.
21 B. S. Murray, *Curr. Opin. Colloid Interface Sci.*, 2007, **12**, 232–241.
22 B. S. Murray, K. Durga, A. Yusoff and S. D. Stoyanov, *Food Hydrocolloids*, 2011, **25**, 627–638.
23 P. A. Wierenga and H. Gruppen, *Curr. Opin. Colloid Interface Sci.*, 2010, **15**, 365–373.
24 T. D. Karapantsios and M. Papara, *Colloids Surf., A*, 2008, **323**, 139–148.
25 M. Papara, X. Zabulis and T. D. Karapantsios, *Chem. Eng. Sci.*, 2009, **64**, 1404–1415.
26 L. M. C. Sagis, *Rev. Mod. Phys.*, 2011, **83**, 1367–1403.
27 J. W. Gibbs, *Collected Works: Volume I Thermodynamics*, Yale University Press, New Haven, 1957.
28 E. H. Laucassen-Reynders, in *Anionic Surfactants: Physical Chemistry of Surfactant Action*, ed. E. H. Lucassen-Reynders, Dekker, New York, 1981, p. 171.
29 H. A. B. Wosten, *Annu. Rev. Microbiol.*, 2001, **55**, 625–646.
30 J. Y. Park, M. A. Plahar, Y. C. Hung, K. H. McWatters and J. B. Eun, *J. Sci. Food Agric.*, 2005, **85**, 1845–1851.
31 E. Dickinson, *Curr. Opin. Colloid Interface Sci.*, 2010, **15**, 40–49.
32 U. T. Gonzenbach, A. R. Studart, E. Tervoort and L. J. Gauckler, *Langmuir*, 2006, **22**, 10983–10988.
33 D. M. Abascal and J. Gracia-Fadrique, *Food Hydrocolloids*, 2009, **23**, 1848–1852.
34 L. J. Lin, P. C. Liao, H. H. Yang and J. T. C. Tzen, *Plant Physiol. Biochem.*, 2005, **43**, 770–776.
35 C. V. Nikiforidis and V. Kiosseoglou, *J. Agric. Food Chem.*, 2010, **58**, 527–532.
36 AOAC, Association of official Analytical Chemists, *Official Methods of Analysis*, Washington, DC, 1994.
37 U. K. Laemmli, *Nature*, 1970, **227**, 680–685.
38 M. A. K. Markwell, S. M. Haas, L. L. Bieber and N. E. Tolbert, *Anal. Biochem.*, 1978, **87**, 206–210.
39 K. Levenberg, *Q. Appl. Math.*, 1944, **2**, 164–168.
40 D. Marquardt, *SIAM J. Appl. Math.*, 1963, **11**, 431–441.
41 G. Loglio, P. Pandolfini, R. Miller, A. V. Makievski, J. Kargel, F. Ravera and B. A. Noskov, *Colloids Surf., A*, 2005, **261**, 57–63.
42 C. V. Nikiforidis and V. Kiosseoglou, *J. Agric. Food Chem.*, 2009, **57**, 5591–5596.
43 M. Millichip, A. S. Tatham, F. Jackson, G. Griffiths, P. R. Shewry and A. K. Stobart, *Biochem. J.*, 1996, **314**, 333–337.
44 M. Ferro, D. Seigneurin-Berny, N. Rolland, A. Chapel, D. Salvi, J. Garin and J. Joyard, *Electrophoresis*, 2000, **21**, 3517–3526.
45 M. Li, D. J. Murphy, K. H. K. Lee, R. Wilson, L. J. Smith, D. C. Clark and J. Y. Sung, *J. Biol. Chem.*, 2002, **277**, 37888–37895.
46 C. V. Nikiforidis and V. Kiosseoglou, *Food Hydrocolloids*, 2011, **25**, 1063–1068.
47 J. T. C. Tzen, G. C. Lie and A. H. C. Huang, *J. Biol. Chem.*, 1992, **267**, 15626–15634.

48 T. Nylander, in *Food Emulsions*, ed. S. Friberg, K. Larsson and J. Sjöblom, CRC Press, New York, 2004.
49 R. Qu and A. H. C. Huang, *J. Biol. Chem.*, 1990, **265**, 2238–2243.
50 E. Roux, S. Baumberger, M. A. V. Axelos and T. Chardot, *J. Agric. Food Chem.*, 2004, **52**, 5245–5249.
51 Y. Gohon, J. D. Vindigni, A. Pallier, F. Wien, H. Celia, A. Giuliani, C. Tribet, T. Chardot and P. Briozzo, *Biochim. Biophys. Acta, Biomembr.*, 2011, **1808**, 706–716.
52 T. D. Karapantsios, V. T. Papoti and G. Doxastakis, *Colloids Surf., A*, 2011, **382**, 74–80.
53 C. V. Nikiforidis and V. Kiosseoglou, *Food Hydrocolloids*, 2007, **21**, 1310–1318.
54 A. Williams and A. Prins, *Colloids Surf., A*, 1996, **114**, 267–275.
55 A. G. Bykov, S. Y. Lin, G. Loglio, R. Miller and B. A. Noskov, *Colloids Surf., A*, 2010, **367**, 129–132.
56 T. B. J. Blijdenstein, P. W. N. de Groot and S. D. Stoyanov, *Soft Matter*, 2010, **6**, 1799–1808.
57 H. B. M. Kopperud and F. K. Hansen, *Macromolecules*, 2001, **34**, 5635–5643.
58 Z. B. Wang and G. Narsimhan, *Langmuir*, 2005, **21**, 4482–4489.
59 N. Alexandrov, K. G. Marinova, K. D. Danov and I. B. Ivanov, *J. Colloid Interface Sci.*, 2009, **339**, 545–550.
60 W. Kloek, T. van Vliet and M. Meinders, *J. Colloid Interface Sci.*, 2001, **237**, 158–166.
61 S. Rouimi, C. Schorsch, C. Valentini and S. Vaslin, *Food Hydrocolloids*, 2005, **19**, 467–478.

